

Contents lists available at ScienceDirect

## Water Research

journal homepage: www.elsevier.com/locate/watres





## Surface-programmed microbiome assembly in phycosphere to microplastics contamination

Xuan Fan <sup>a</sup>, Lingyu Kong <sup>a</sup>, Jingyi Wang <sup>a</sup>, Yixiao Tan <sup>a</sup>, Xiangyang Xu <sup>a,c</sup>, Mengyan Li <sup>d</sup>, Liang Zhu <sup>a,b,c,\*</sup>

- a Department of Environmental Engineering, Zhejiang University, Hangzhou 310058, China
- b Innovation Center of Yangtze River Delta, Zhejiang University, Jiashan 314100, China
- <sup>c</sup> Zhejiang Provincial Engineering Laboratory of Water Pollution Control, 388 Yuhangtang Road, Hangzhou 310058, China
- d Department of Chemistry and Environmental Science, New Jersey Institute of Technology, Newark, NJ 07102, United States

### ARTICLEINFO

### Keywords: Algae-bacteria symbiotic system Microplastics Phycosphere interactions Chemotaxis Biodegradation pathway

### ABSTRACT

Recalcitrance in microplastics accounts for ubiquitous white pollution. Of special interest are the capabilities of microorganisms to accelerate their degradation sustainably. Compared to the well-studied pure cultures in degrading natural polymers, the algal-bacterial symbiotic system is considered as a promising candidate for microplastics removal, cascading bottom-up impacts on ecosystem-scale processes. This study selected and enriched the algae-associated microbial communities hosted by the indigenous isolation Desmodesmus sp. in wastewater treatment plants with micro-polyvinyl chloride, polyethylene terephthalate, polyethylene, and polystyrene contamination. Results elaborated that multiple settled and specific affiliates were recruited by the uniform algae protagonist from the biosphere under manifold microplastic stress. Alteration of distinct chemical functionalities and deformation of polymers provide direct evidence of degradation in phycosphere under illumination. Microplastic-induced phycosphere-derived DOM created spatial gradients of aromatic protein, fulvic and humic acid-like and tryptophan components to expanded niche-width. Surface thermodynamic analysis was conducted to simulate the reciprocal and reversible interaction on algal-bacterial and phycosphere-microplastic interface, revealing the enhancement of transition to stable and irreversible aggregation for functional microbiota colonization and microplastics capture. Furthermore, pangenomic analysis disclosed the genes related to the chemotaxis and the proposed microplastics biodegradation pathway in enriched algal-bacterial microbiome, orchestrating the evidence for common synthetic polymer particles and ultimately to confirm the effectiveness and potential. The present study emphasizes the necessity for future endeavors aimed at fully leveraging the potential of algal-bacterial mutualistic systems within sustainable bioremediation strategies targeting the eradication of microplastic waste.

### 1. Introduction

Human activity produces enormous plastic pollution on a global scale (Waters et al., 2016). Polyethylene (PE), polyvinyl chloride (PVC), polystyrene (PS) and polyethylene terephthalate (PET) constitute about 80 % of the total global plastic usage (Phuong et al., 2016; Wilkes and Aristilde, 2017). The concurrent prevalence of microplastic pollution has catastrophic impacts, jeopardizing aquatic ecosystems worldwide (Santos et al., 2021). Dissimilar to sizable plastic waste, the microbeads in aquatic environments precludes their effective retrieval for recycling or systematic mitigation. Microplastics primarily originate from the

discharge of untreated sewage originating from wastewater treatment plants (WWTPs) (Strokal et al., 2021; Woodward et al., 2021), which are recognized as the source and export of microplastics to terrestrial and marine environment (Syranidou and Kalogerakis, 2022) and concentrate copious microplastics from urban areas (Kay et al., 2018). Previous studies have reported the release of 300 million plastic debris per day from a WWTP (Edo et al., 2020). Currently, there are no regulations pertaining to the microplastics in effluents and sewage sludge or their mitigation during wastewater treatments (Freeman et al., 2020).

The inherent resistance of polymers makes degradation process of microplastics in environmental matrices sophisticated and arduous

<sup>\*</sup> Corresponding author at: Department of Environmental Engineering, Zhejiang University, No. 866 Yuhangtang Road, Hangzhou 310058, China. *E-mail address*: felix79cn@zju.edu.cn (L. Zhu).

(Andrady, 2017). Recently, biodeterioration, biofragmentation, and mineralization of microplastics has been observed. Miscellaneous pure isolates of actinomycetes (Auta et al., 2018), bacteria (Sun et al., 2022; Yoshida et al., 2016), fungi (Russell et al., 2011; Sánchez, 2020) and algae (Cheng and Wang, 2022) with the potential to biodegrade various plastic polymers were researched. However, the high diversity and niche width of microorganisms across different natural habitats has not been significantly exploited vet (Amobonye et al., 2021). Indeed, evidence from theoretical and laboratory-based studies indicated that microbial communities were more effective in degrading natural polymers and xenobiotics than pure cultures (Giacomucci et al., 2020; Vargas-Suárez et al., 2019; Zafar et al., 2013). An increasing cohort of researchers is placing their optimism in algae-bacterial symbiotic system for environmental purification with the advantages of photosynthetic efficiency, eco-friendliness and self-defensive (Lin et al., 2021; Song et al., 2020; Yong et al., 2021). A multitude of studies have documented the deleterious effects of small-sized microbeads on algae (Liu et al., 2020; Wu et al., 2019), as well as the interactions between microplastics and algae (Feng et al., 2020; Thiagarajan et al., 2019), or bacteria (Di Cesare et al., 2024). Nevertheless, limited research has delved into the fate of microplastics within the algae-bacteria symbiotic system (Huang et al., 2022a) and whether these pollutants could potentially impact on the phycosphere interface (Jia et al., 2023). This interdependence between microplastics and microbe in phycosphere signified a pivotal influence on ecosystem function and climate-relevant chemical fluxes (Amin et al., 2012; Seymour et al., 2017), facilitating microbial colonization (Seymour et al., 2017) and microplastics capture (Gonzalez-Fernandez et al., 2019), thereby initiating the process of plastic biodegradation.

Considering the intrinsic physical and chemical features of this unique aquatic microenvironment, relating these characteristics to other analogous systems is informative (Seymour et al., 2017) for further comprehension of phycosphere handling with xenobiotic pollutants, e. g., microplastics. Akin to reversible bacterial adhesion to a substratum surface (Carniello et al., 2018) and directed cell migration (Cremer formulated 2019), numerical approaches chemotaxis-mediated and spatiotemporally transient associations occurred within the phycosphere (Raina et al., 2023). Although the fleeting and repeat encounters providing a viable strategy for nutrient exchanges in aquatic ecosystems (Raina et al., 2023; Seymour et al., 2017; Smriga et al., 2016), the consequent transition from labile and reversible to stable and irreversible of algal-bacterial relationship is of global significance within the context of ecosystem function. Overcoming the limitation in researching surface-programmed microscale hetero- and homo-interactions over bond-strengtheningtime-scales (Carniello et al., 2018) is imperative.

This study aimed to explore the presence of a shared degradation pathway for common microplastics (PVC, PET, PE, and PS) through algal-bacterial consortia within sewage treatment systems. Herewith, we isolated the autochthonous algae, *Desmodesmus* sp. IPPAS S-2014, from a full-scale WWTP to construct the potential microplastics-degrading aggregation. Multidisciplinary methods were applied to characterized the degradation of polymers, consisting of unique characteristic band and deformation. We integrated the traditional physicochemical approaches with genomic evidence of chemotaxis to yield a comprehensive paradigm of algal-bacterial and phycosphere-microplastic interactions with the goal of delivering the fresh perspective on surface-programmed microenvironment. Additional pangenomic analysis rendered assistance to postulated the plausible degradation mechanisms to verify the potential of enriched algal-bacterial consortia to microplastics contamination.

### 2. Materials and methods

## 2.1. Incubations and microbial isolation from wastewater treatment

A schematic depicting the experimental setups (the Section 2.1 and 2.2) was found in Figure S1. For incubations, activated sludge were collected from a full-scale wastewater treatment plant in Hangzhou, China. Algal samples were obtained from the sidewall of secondary sediment tank of the same WWTP. The samples were transported to the laboratory and stored at 4 °C. The algae-bacteria consortium used for incubations was a mixture of the activated sludge and algae (1:1 v/v). Tissue culture flasks (25 cm<sup>2</sup>) containing 25 mL of BG-11 medium, supplemented with each one of four microplastics (100 mg PVC, PET, PE or PS with diameters of 75 um, purchased from Huachuang Plastic Inc., Dongguan, China), were inoculated with 1 mL of the natural algaebacteria consortium. The concentration of microplastics was approximately equal to 10<sup>5</sup> particles/L, environmentally relevant to representative amount of microplastics in the sewage sludge (Li et al., 2018). The microplastics were sterilized by washing three times with 75 % ethanol and then dried in a biosafety chamber under UV light. A total of two treatments were prepared: 1. Activated sludge + algae + BG11 + microplastics (AS-PVC/PET/PE/PS); 2. Algae + BG11 + microplastics (A-PVC/PET/PE/PS). Cultures were incubated at 25 °C under 12-h light and 12-h dark cycles, with an illumination intensity of 15,000 lux during the light period, with shaking at 150 rpm. After approximately 4 weeks, 1 mL of these cultures was used to inoculate fresh tissue culture flasks (25 cm<sup>2</sup>) with 25 mL of BG11 media, as above, in a second enrichment step. Agar plates were made with the BG-11 medium, containing 4 mg/ml of one of the microplastics listed above and 1.5 % agar. Media were blended immediately before pouring the plates to ensure homogeneous dispersal of the microplastics. 100 uL of the second enrichment cultures was spread on to replicate plates and incubated for 3 weeks. According to co-occurrence network analysis (see the Section 3.1 for details), a putative microplastics-degrading algae strains were isolated, affiliated with Desmodesmus (Desmodesmus sp. IPPAS S-2014, see the Section 2.5).

### 2.2. Phycosphere enrichment

Algae–bacteria consortium (referred to as "phycosphere enrichments") were obtained from laboratory enrichments of *Desmodesmus* sp. IPPAS S-2014 and maintained as previously described (Jackrel et al., 2021; Kimbrel et al., 2019). Briefly, the second enrichment cultures were filtered with 0.6–1  $\mu m$  pores to remove larger algae cells. The bacterial filtrates were inoculated to algae culture, maintained in BG-11 media and washed with a sterile medium to enrich for phycosphere-associated bacteria. These enriched communities were subsequently co-cultured with *Desmodesmus* sp. IPPAS S-2014 in BG-11 media and transferred 5 times every 2 weeks, ensuring that the reflect members were subsisting on algal-derived organic matter, prior to the start of the experiments (Sjöstedt et al., 2012). For next analysis, phycosphere enrichments were centrifuged at 3000  $\times$  g 3 times to obtain phycosphere-associated bacteria and free-living bacteria.

## 2.3. Identification of the microplastic degradation

The microplastics were rinsed and pre-treated aseptically before measurement (Text S1). Functional group types and contents of microplastics were measured by FT-IR (NicoLET iS50FT-IR, Thermo Scientific, USA) with the wavenumber range of 400 to 4000 cm<sup>-1</sup>. Additional treatment of microplastics in BG11 media was set to avoid the effects of illumination and media (Sun et al., 2022). The microbial aggregates modified AFM probes were used to determine the surface topography, adhesion forces and Young's Modulus of microplastics by an AFM force spectroscopy (Dimension ICON, Bruker, Germany) at the nanoscale level

(Text S2) (Xu et al., 2024). The morphology of microbial colonization and corrosion on the microplastics surface were visualized by scanning electron microscopy (SEM, Sigma 300, Zeiss, Germany).

### 2.4. Analysis of phycosphere-derived EPS

Extracellular polymeric substances (EPS) including tightly bound (TB), loosely bound (LB), and soluble(S) EPS was extracted by the heating method (Zhang et al., 2018). Concentrations of protein (PN) and polysaccharide (PS) in EPS were determined by BCA Kit Method and phenol sulfuric acid method (Dubois et al., 1956). EPS components were measured by the three-dimensional excitation-emission matrix (3D-EEM) fluorescence spectrometer (F-4500 FL, Hitachi). Phycosphere-derived dissolved organic matters (DOM) were separated by the parallel factor (PARAFAC) analysis of EEM spectra data in R (version 4.3.0) with the package "staRdom" (Text S3) (Tan et al., 2023). The DOM landscape was modeled through the diffusion equation (Text S4) (Raina et al., 2023).

### 2.5. Surface thermodynamic analysis for interactions

All kinds of microplastics and microbial aggregates were previously characterized in terms of contact angles and the surface Zeta potentials for measuring the surface energies. Contact angles of double distilled water, glycerin, diiodomethane and formamide (>99.5 %, Sigma–Aldrich, USA) on the surface were determined by the sessile droptangent method using a drop shape analysis system (Theta Lite, Finland) at room temperature ( $25\pm1~^{\circ}$ C) according to our previous works.(Ji et al., 2023) Prior to contact angle measurement, the samples were introduced on glass slides after vacuum filtration and then air-dried for 30 min (Ou et al., 2020; Yuan et al., 2018). Zeta potentials and the particle size were determined using Zetasizer (Nano ZS90, Malvern, UK). Heteroaggregation and homo-aggregation of phycosphere and microplastics were observed via QICPIC dynamic image analysis system (Sympatec GmbH, Germany).

The Surface thermodynamic theory was applied to calculate the interaction energy on algal-bacterial and phycosphere-microplastic interface. The total interaction energy was basically composed of Lifshitz-van der Waals energy, electrostatic force and acid-base interaction energy as proposed by van Oss (1993). The detailed calculation process was described in the Supporting Information (Text S5).

### 2.6. DNA sequencing and analysis

As previously described (Tan et al., 2023), DNA was extracted from phycosphere enrichment samples using Qiagen DNeasy PowerSoil Kits. The samples were sent to Sangon Biotech, Shanghai. for 16S rRNA and 18S rRNA gene sequencing and then built co-occurrence networks via R (version 4.3.0). The binning procedures of the metagenome libraries followed the protocols in previous publications (Tan et al., 2023). Briefly, the assembled contigs of each sample were binned by meta-WRAP (version 1.2.2) and estimated by CheckM (version 1.0.12), with completeness <50 % or contamination >10 % discarded. GTDBTk (https://github.com/Ecogenomics/GtdbTk) was applied for assignment taxonomy for each metagenome assembled genome (MAG). MAGs associated with the putative microplastic-degraders were downloaded from the EggNOG database (version 5.0) for pangenomic analysis. Enzymes, related protein, and pathways in proposed microplastics biodegradation and bacterial chemotaxis progress was referred to the Kyoto Encyclopedia of Genes and Genomes (KEGG) databases (https://www.kegg.jp). Then,  $\alpha$  and  $\beta$ -diversity estimation were performed using the R. The phylogenetic tree was generated by GTDB-Tk (version 2.1.1) module "de\_novo\_wf" based on the database Genome Taxonomy Database (http://gtdb.ecogenomic.org, Release207), visualized in iTOL (https://itol.embl.de) (Text S6).

### 2.7. Statistical analysis

SPSS 18 software (SPSS Inc., USA) was applied to carry out T-test and Pearson correlation analysis (two-tailed test) and a p-value of <0.05 was accepted as statistical significance. The calculations and drawing of profiles of the interaction energies on the separation distance were performed in OriginPro software (version 9.0.0). GraphPad Prism (version 9.5.1) was to visualize the rest of the data. All experiments were conducted in at least three replicates and the data represents the mean values  $\pm$  standard error.

### 3. Results and discussion

### 3.1. Selection of microbiomes to microplastics contamination

### 3.1.1. Initial source communities from WWTP

The structure of microbial communities in initial and microplasticinduced phycosphere communities were analyzed. The algae phylum distribution of the bacterial communities in the mixed-species communities were primarily Chlorophyta, Bacillariophyta and Streptophyta, with <5 % in the reads of eukaryote phyla (Figure. S2a). Bacillariophyta were dominant in the origin algae-bacterial consortia. The bacterial microbiomes of phycosphere communities obtained from the sidewall of the secondary sediment tank were primarily comprised of Proteobacteria (mean 50.29 % for AS/A- PVC/PET/PE/PS) followed by Cyanobacteria (mean 23.31 % for AS/A-PVC/PET/PE/PS) at the phylum level (Figure. S2b). Microplastic-induced facilitated the absolute predominance of Chlorophyta (mean 93.81 %) of eukaryote algal in initial source communities (Figure S2c). The abundant taxa Cyanobacteria and Proteobacteria remained greater robustness (mean 94.67 %, Figure S2d), signifying that the succession of bacterial microbial community conformed to the so-called "Matthew effect" under microplastic stress (Merton, 1968).

Considering algal-bacteria interactions are multifarious and often highly sophisticated (Seymour et al., 2017), co-occurrence analysis of the algae-microbiome network containing 3 modules, was manifested. Modules were heterogeneous in terms of diversity, with module 1 comprising Stramenopiles sp. and Chrysophycase sp. algal microbiome, module 2 and 3 including Parachlorella kessleri and Nitzschia patea algal microbiome, respectively (Fig. 1a). The secondary sediment tanks of WWTP are open to the environment and thus under constant exposure to invading bacteria and eukaryotes that may not all be directly utilizing algae exudates and eventually constructing the phycosphere to a certain contamination (e.g., microplastics). Each network community had a considerable proportion of new members, and the complexity and robustness of ecological networks diminished with stronger transmissibility exposed to microplastics (Fig. 1b). The Chrysophyceae, Desmodesmus, Chlorella and Kumanoa algal microbiome were still in the ascendant, underpinning the high robustness of algae-dominated communities. Collectively, much denser algal-bacterial interactions were formed and convergent selection of specific taxa in phycosphere was intensified. Furthermore, giving that the combined score of high mean degree (0.280), high closeness centrality (0.423) and low betweenness centrality (0.035, Fig. 1c and Table S1) should be used as a threshold for defining keystone taxa in microbial communities (Banerjee et al., 2018), alternative to the competitive lottery hypothesis, or in combination with it, we hypothesized Desmodesmus sp., as the algal host, was actively selecting for the community members through the production of bioactive compounds under microplastic stress. In accordance with the shifts in taxonomic composition of the biosphere, microbial diversity declined significantly (p < 0.05) with microplastic stress considering niche width and overlap (Fig. 1d).

## 3.1.2. Desmodesmus exudate enrichments

Although the *Desmodesmus* genus has not been reported to degrade microplastic and polymer, we were interested in recruiting the bacterial

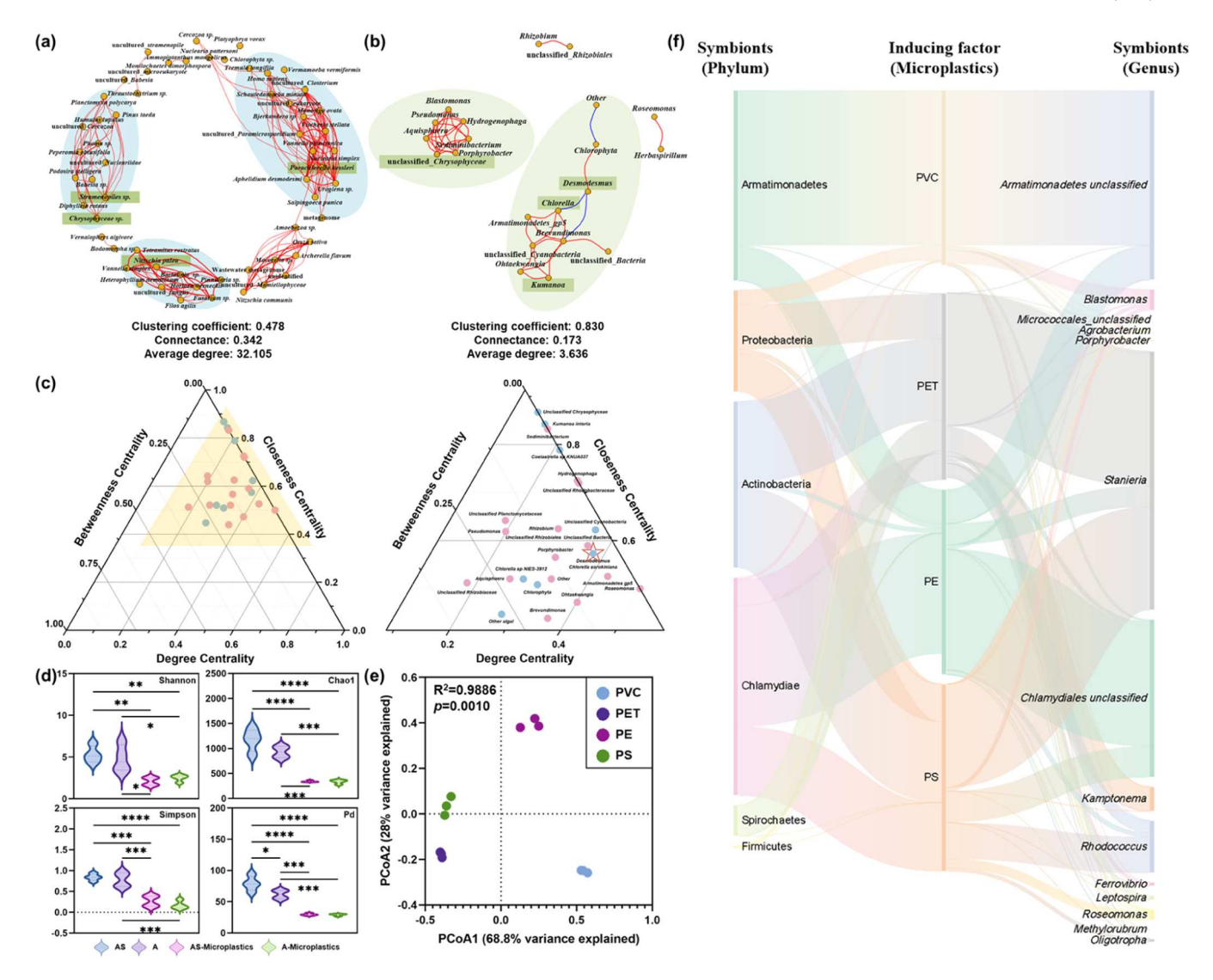


Fig. 1. Overview of the microbes inhabiting algal-bacterial consortia. Co-occurrence networks of (a) seeding and (b) microplastic-inducing algae–bacteria consortium. (c) Ternary plot of degree centrality, closeness centrality and betweenness centrality of microplastic-inducing microbiota. Right panel is the partial enlarged detail of the left panel. (d) α-Diversity. Asterisks refer to the significance estimated by Student's test, \*\*p < 0.01, \*\*\*p < 0.001, and \*\*\*\*p < 0.0001. (e) β-Diversity. (f) Microbial compositions in *Desmodesmus* sp. IPPAS S-2014 exudate enrichments.

communities from the wastewater samples to those members able to subsist solely in Desmodesmus-derived phycosphere to identify microplastic-degrading algal-bacteria consortia in the current study. Thus, we generated four exudate enrichments with source bacterial communities from AS/A- PVC/PET/PE/PS microbiome inoculated into isolation of Desmodesmus strain, Desmodesmus sp. IPPAS S-2014, for laboratory batch cultures. After several transfers, principal co-ordinates analysis (PCoA) revealed that the microbial compositions of potential microplastic-degrading algal-bacteria symbiotic system with host selection varied significantly between different polymer treatments  $(R^2=0.9886, p=0.0010, Fig. 1e)$ , unlike that of pre-remodeled microbial communities (Figure S2e). Particularly, microbes identified in PET and PS-induced treatments both exhibited Stanieria (70.71  $\pm$  1.94 % and  $55.23 \pm 6.42$  %, respectively) dominated structure, while Armatimonadetes (83.02  $\pm$  4.52 %) and Chlamydiales unclassified genera outcompeted in PVC and PE-induced consortia, respectively (Fig. 1f and S2f). Previous studied demonstrated the influence of the algal host in directing bacterial community composition to a greater degree than other environmental factors (Jackrel et al., 2021; Kimbrel et al., 2019). Nevertheless, members recruitment of identical algal host, Desmodesmus sp. IPPAS S-2014, from microplastic-induced algal-bacterial biosphere with different polymer disturbance, contribute the divergence towards phylogenetically and functionally disparate states.

## 3.2. Evidence of MP degradation in phycosphere under illumination

In this study, we applied microplastic-media treatment to distinguish whether the variations of polymer were account for biodegradation or for photochemical behavior and media. Functional groups within plastic polymers were examined using FT-IR spectroscopy to detect alterations on the surface of microplastics and to assess the degradation process resulting from microbial colonization (Fig. 2) (Jung et al., 2018; Sun et al., 2022; Wang et al., 2022).

There was a substantial decrease in the absorption intensity of CH $_2$  rock (~966 cm $^{-1}$ ) and an existence of C-O-C stretch (1270~1010 cm $^{-1}$ ) on PVC in phycosphere. An alternative explanation that CH $_2$  rock coupled with C-C stretch (~1099 cm $^{-1}$ ) led to the frequency deviation. The degradation process slashed C=O stretch (~1713 cm $^{-1}$ ), C-O stretch (~1241 and 1094 cm $^{-1}$ ) and aromatic CH out-of-plane bend (~720 cm $^{-1}$ ), which are mode assignments for FT-IR spectra of PET, while contributed to the formation of C=O stretch (~1634 cm $^{-1}$ ) and CH $_3$  bend (~1377 cm $^{-1}$ ) as the intermediate products. Formation of functional

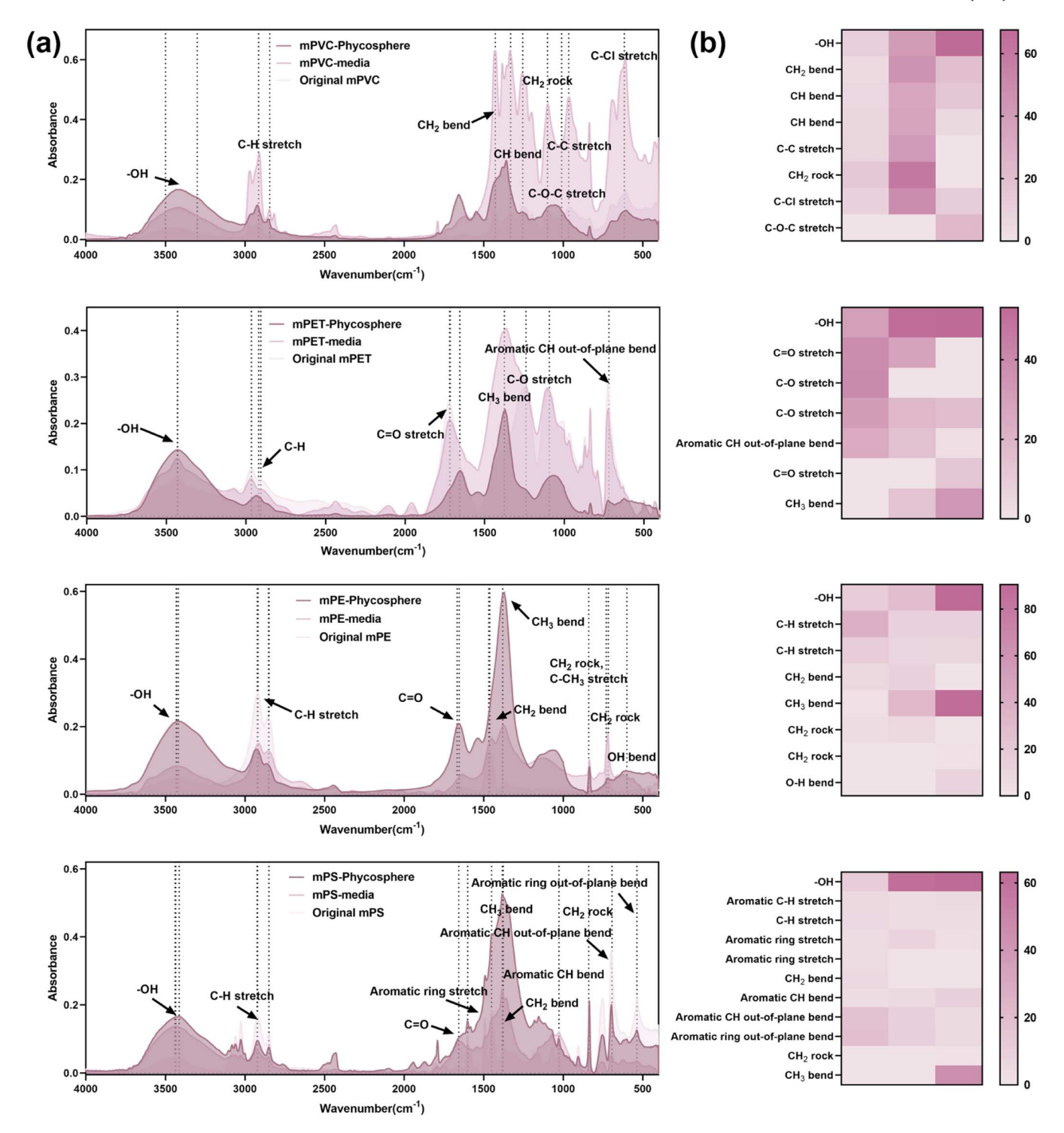


Fig. 2. FT-IR analysis of original microplastics, microplastic-only and microplastic + algal microbiomes treatment. (a) Absorbance spectrum between wavelength 4000 to 400 cm-1 were visualized. Characteristic absorption bands (cm-1) used to identify each polymer were marked. (b) Heatmap compared the assignments for the FT-IR spectra of microplastics identified. The ribbons referred to original microplastic, microplastic-media and microplastic-phycosphere from left to right.

groups,  $-OH~(3300-3500~cm^{-1})$ ,  $CH_3~bend~(\sim1377~cm^{-1})$  display significant peaks, with emerging  $CH_2~rock$ ,  $C-CH_3~stretch~(\sim840~cm^{-1})$  and  $O-H~bend~(\sim600~cm^{-1})$  on PE after biodegradation. Analogously,  $CH_2~rock$ ,  $C-CH_3~stretch~(\sim840~cm^{-1})$  and  $CH_3~bend~(\sim1377~cm^{-1})$  turned primary on PS in phycosphere.

Principal component analysis (PCA) scatter plots (Figure S3a) articulated that microplastics were significantly distinguished in potential microplastics-degrading algal microbiomes ( $R^2$ =0.3780, p = 0.0030). Furthermore, combining the influence on two principal components,

oxygen-containing groups, C=O and C-O-C stretch were responsible for these classifications of PVC,  ${\rm CH_3}$  bend for PET, PE and PS (Figure S3b), on account of the proportion of oxidation and depolymerization reactions in the biodegradation via algal-bacterial system. This evidence supports our ability to predict and identify the production of intermediates in the degradation process.

Besides, surface properties revealed by AFM and SEM also elucidated the erosion and weathering of microplastics via degradation in phycosphere (Figure S4). The formation of pit plugs and significantly reduced Young's modulus signified the break in the backbone and fragility of polymers (Figure S4ab) (Lou et al., 2023; Wu et al., 2023). Microbial intrusion augmented the biodeterioration and biofragmentation of polymers and formed the plastisphere embracing spherical aggregate (Figure S4c).

# 3.3. The spatial gradients of microplastic-induced phycosphere-derived DOM

Phycosphere, framed by EPS, posits that organic matter exuded by algal cells forms spatial gradients conducive to selective bacterial colonization. As the primary information on the phycosphere-derived EPS provided via the EEM spectra (Fig. 3a), migration of principal components in fluorescent DOM were explicitly observed considering interior and exterior spatial regions of phycosphere. It seemed that DOM assignments were highly conserved under various microplastic materials, uniquely shaped by spatial arrangement in EPS and algal-host (Figure S5 and S6a). Three fluorescence components (C1 at Ex/ Em=225/310 nm, C2 at Ex/Em=280/340 nm, C3 at Ex/Em=260/440 and 335/440 nm) could be identified from DOM of potential microplastic-degrading phycosphere (Fig. 3a). Thereinto, component 1, related to aromatic protein I, and component 2, referred to tryptophan and protein-like components, respectively, demonstrated a decreasing trend from suspended to bound-EPS in all microplastic-treatments (Fig. 3b), confirming a spatial gradient of phycosphere-derived with increasing distance from the cell surface. However, fulvic and humic acid-like components (C3) abounded in tightly bound from nonexistence in soluble EPS. These results were at odds with distribution of DOM in original aggerates (Figure S6). Compound-class composition of DOM fractions was more sophisticated for additional aromatic protein II (Ex/ Em=220/346 and 280/346 nm) and humic acid-like components (Ex/ Em=255~330/410 nm) were ascertained. Reverse trends of aromatic protein I and tryptophan components appear (Figure S5c). The

diminished spatial gradients of organic matters exuded within the phycosphere fostered niches sustaining at least 3 bacterial lifestyles, thereby alleviating limiting resources competition for selected microplastic-tolerant bacterial. The first and second niches supported bacteria that exclusively responded to the component 1 and 2 concentration gradients, thriving best in locations farthest from the algal cells. The third niche harbored bacteria that utilized fulvic and humic acid-like components for growth, potentially indicating their survival in closest proximity to the algae.

It had been reported that environmental biofilms matrix can contain considerable amounts of proteins that, together, can far exceed the polysaccharide content, on a mass basis (Flemming and Wingender, 2010), whereas exudate of *Desmodesmus* sp. enrichments possessed exopolysaccharide-dominated EPS structure (Fig. 3d), which was consistent with the theoretical property of phycosphere. Exopolysaccharides involved in the adherence to abiotic and biotic surfaces, e.g., algal-bacterial, and phycosphere-microplastic interface, and in the maintenance of biofilm architecture, thus, furnishing the attachment and biodegradation of microplastics with a competent platform. Also, exopolysaccharide potentially imparted the microplastic-tolerance to the enriched species assemblage.

## 3.4. Microplastics-induced reversible phycosphere interactions

Evidence for substantial complexity and sophistication in the chemical exchanges between algae and bacteria is suggestive of a requirement for close spatial proximity of the protagonists (Kim et al., 2022; Seymour et al., 2017). Phycosphere interactions has been documented be short-lived yet repeated (Raina et al., 2023), which coincided with the classical and extended surface thermodynamics that bacteria was generally assumed to adhere reversibly at a secondary minimum energy discerned (Carniello et al., 2018). Accordingly, physico-chemical models were applied to disclose the interactions between diversity

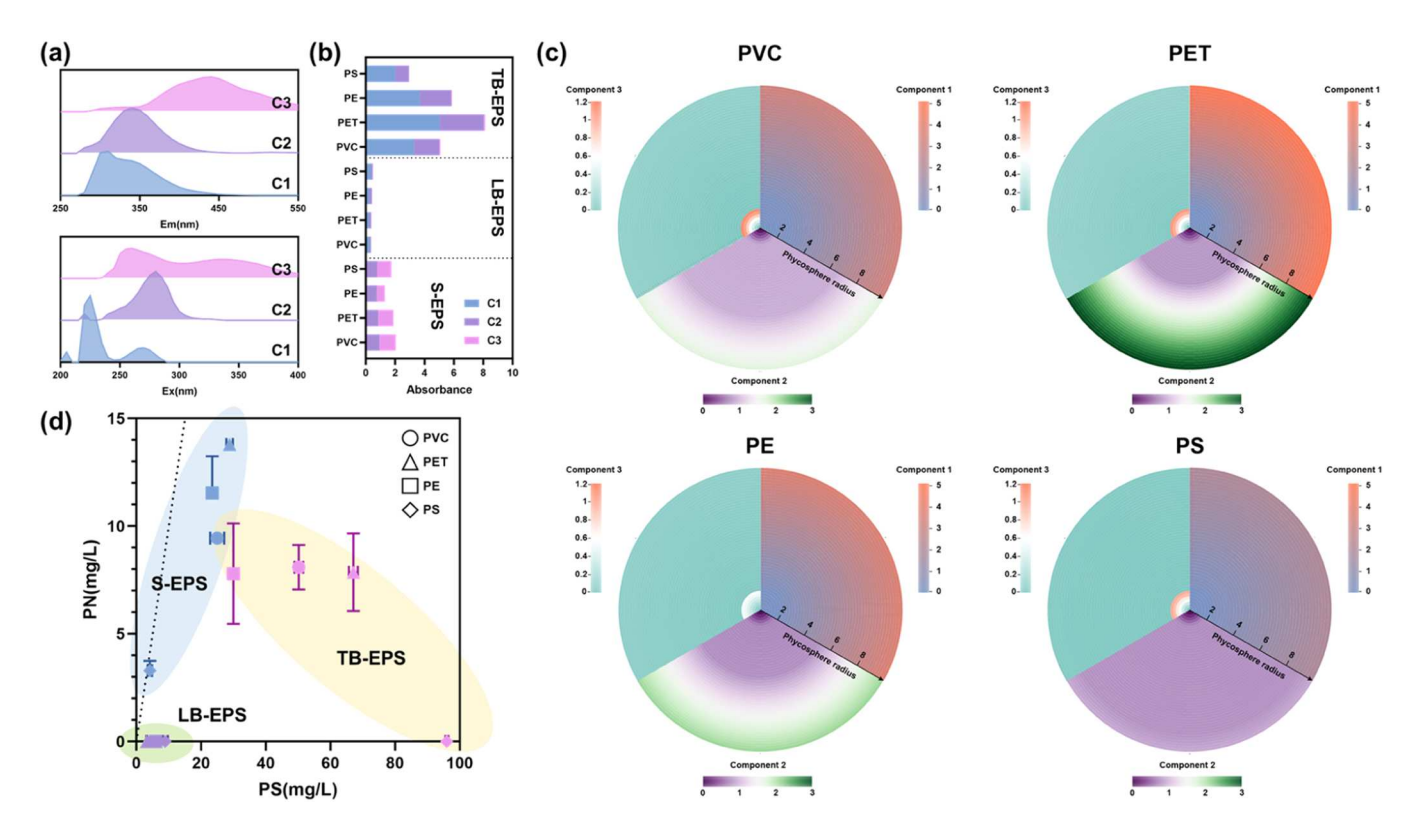


Fig. 3. Characteristic of phycosphere-derived EPS. (a) Three main components (1, 2, and 3, respectively) in EPS extracted from PARAFAC analysis; (b) The distribution of each EEM-PARAFAC component in DOM released from enriched algal-bacterial consortia. (c) The spatial gradients of microplastic-induced phycosphere-derived DOM. The phycosphere radius was measured in the diameter of the innermost layer (TB-EPS). (d) PN and PS concentration in EPS.

interface containing algal-bacterial and phycosphere-microplastic boundary surface (Fig. 4). It was worth mentioning that the insurmountable potential energy barrier defined in the ideal model occurred at the minimum separation distance ( $y_0$ =0.158 nm) (Kim and Hoek, 2007) in this study, therefore, the energy barrier was excluded from the discussion herein.

### 3.4.1. Algal-bacterial interface

Pursuant to the conceptual simulation (Carniello et al., 2018), the region where the algal-derived organic nutrients (phycosphere) is regard as the substratum surface, orchestrating the biofilm-inhabitants adhesion, as programmed by the physico-chemistry algal-protagonist surface. Hence, we antecedently assumed the algal-bacterial interaction patterns were undisturbed by the existence of microplastics, namely cell-cell direct physical proximity occurred automatically. Natheless, homo-aggregation in phycosphere interactions was unfavorable (interaction energy > 0) in most physical space between the two partners referring to surface thermodynamics (Absolom et al., 1983), declaring polymers had participated in and complicated the algal-bacterial interaction pattern. Intermittent algal-bacterial contacts proceeded in the region with a separation distance of 1.84, 3.30, 4.66 nm in PVC, PET and PE-treatments, respectively, while irreversible adhesion was maintained under PS added.

Previous studies suggested reversibly adhering bacteria were confined in the secondary energy minimum (i.e., the minimum energy in this manuscript), and more reversibly binding tethers couple a bacterium irreversibly with a substratum surface (Carniello et al., 2018). On the strength of theoretical basis, it was inferred that the transition from reversible to irreversible adhesion to algal-host were enhanced, quantified as  $\infty$ (PS)>>8537.92 kT (PVC) > 3482.76 kT (PET) > 1876.85 kT (PE), confirming a response of phycosphere interactions to microplastics contamination. Pearson correlation analysis confirmed the contribution of S-EPS production to strengthening of the bacterium-substratum bond (p < 0.05, R<sup>2</sup>=0.971) as previous literatures (Chao and Zhang, 2011; Pranzetti et al., 2013). Phycosphere-associated bacterial was inferred to localize in the outer layer.

## 3.4.2. Phycosphere-Microplastic interface

Furthermore, with respect to the self-assembly and homoaggregation of microplastic and algal-bacterial associations (Figure S7 and S8), we hypothesized there were two modes for phycospheremicroplastic interaction: (1) Heteroaggregation of microplastics and the algal-bacterial aggregates; and (2) Microorganisms attachment on the microplastics in the form of biofilms, i.e., plastisphere. Considering the first scenario, significant micro-PVC, PET and PE deposition occurred in the secondary energy minimum (Hahn and O'Melia, 2004) with the distance of 4.16, 19.04 and 5.53 nm, respectively. Moreover, given that 1.5 kT as the thermal energy of a colloidal particle (van der Westen et al., 2018), these polymer particles were captured on a substantial scale quantified as 216,510.09 kT (PVC) >176,152.98 kT (PET)>93,138.42 kT (PE), which signified that adsorption was a prior and pivotal step in the degradation of microplastics in Desmodesmus sp. exudate enrichments (Fig. 4c) (Gonzalez-Fernandez et al., 2019). Analogously, microplastics were suggested to interacted with tryptophan and protein-like components in the soluble layer (p < 0.05, R<sup>2</sup>=0.974), which aligned with the aggregation kinetics regrading microplastics in aquatic environment influenced by their interactions with manifold proteins (Huang et al., 2022b).

In the latter postulated pattern, algal and bacterial were transported towards the microplastic surface, thus formed the so-called plastisphere (Amaral-Zettler et al., 2020). The development of plastisphere conformed to the traditional biofilm formation (Zettler et al., 2013). Under this circumstance, distinct physico-chemically controlled steps of microbial aggregates settlement on PVC and PET surface were zooming in beyond the distance of 1.23 and 1.77 nm, respectively. Irreversible adhesion on PE maintained stability (Fig. 4d). Particularly, it's

struggling for close physical proximity of PS on PS-induced phycosphere within a distance greater than 0.49 nm as well as microbial attachment on PS surface. Supplemented with adhesion force and interactions on the microplastic-bacterial interface (Figure S8hij), we hypothesized the sequence of the algae and bacteria deposition that bacterial as the pioneer attached on the microplastic foremost, followed by the algae cells. The results might explain the deviation of host selection that bacterial communities varied under different microplastic-stress recruited by the same algal host. The hypothesis was verified and visualized via SEM (Figure S4c), rendering algal-bacterial consortia enfolding the polymer debris and conglobate microbial assemblages encircling the microplastics.

Cell motility incurs an energetic expense (Ni et al., 2020) that has been not explicitly considered in phycosphere previously. High energetic cost of reversible adhesion (Carniello et al., 2018) would offset fitness benefit (Ni et al., 2020; Raina et al., 2023). The presence of microplastics expanded the phycosphere interaction zone and allowed the transition from a reversible to a more irreversible state of contacts, enlarging the ecological niche simulated via physico-chemical mechanisms. Besides, the microplastic-phycosphere interface shifted with the degradation process: initially, microorganisms formed plastisphere on the polymer surface; and then microplastics biodegraded with smaller particle size absorbed onto the barrier region of mature algal-bacterial consortia.

### 3.5. Chemotaxis involved in phycosphere interactions

In addition to direct cell-to-cell adhesion, phycosphere interactions between algae and bacteria frequently manifest as bacterial chemotaxis toward spatial gradients of algal-derived nutrients (Kim et al., 2022). Chemotaxis strongly affects unique and repeated phycosphere encounters (Raina et al., 2023). Consequently, coupling the comparative gene-centric and genome-resolved metagenomics, we unraveled the potential metabolic mechanism resulting in microscale interactions (Fig. 5).

Proteobacteria and an unclassified taxa-derived methyl-accepting chemotaxis proteins (tsr and tar) were up-regulated significantly by  $11.53\sim11.98$  folds. In the light of molecular mechanisms of chemotaxis, microplastic-inducement reinforced the sense of the environmental stimuli via the chemosensory proteins, tsr and tar, embedded in the cytoplasmic membrane (Tajima et al., 2011). Armatimonadetes and Gemmatimonadetes-dominated gene encoding chemotaxis protein (CheC) increased 9.07~12.81-fold, indicate the strengthening of microplastic-induced niche adaptation and signal termination (Park et al., 2004) and further colonization and co-existence of bacterial in phycosphere (Laganenka et al., 2023). The chemotaxis paradigm of potential microplastics-degrading algal-bacterial consortia tended to be the combination of the traditional E. coli and Bacillus subtilis models (Laganenka et al., 2023; Ni et al., 2020; Park et al., 2004) for emerging regulation of CheC herein. The bacterial chemotaxis in phycosphere was divorced from the fimbriae in consideration of the bare enrichment of genes encoding switch protein of the flagellar motor, FliG, FliM and FliN (Figure S9), which markedly diminish cell growth.

Host-derived microorganisms in phycosphere exhibit heterogeneous spatial distribution, enabling niche segregation and facilitating stable co-existence of species with multi-faceted metabolic preferences (Laganenka et al., 2023). Chemotaxis potentiates motile bacteria to navigate in chemical gradients (Fig. 3c) and facilitate metabolic exchanges (Colin and Sourjik, 2017; Laganenka et al., 2023; Milo et al., 2010; Ni et al., 2020; Raina et al., 2023) and colonization of beneficial niches by free-living and host-associated bacteria (Laganenka et al., 2023; Matilla and Krell, 2018). This regulation tactic of optimizing the related protein (tsr, tar and CheC) was primarily a consequence of higher investment into the chemotaxis for the adaptability to environmental disturbance and biodegradation of microplastics.

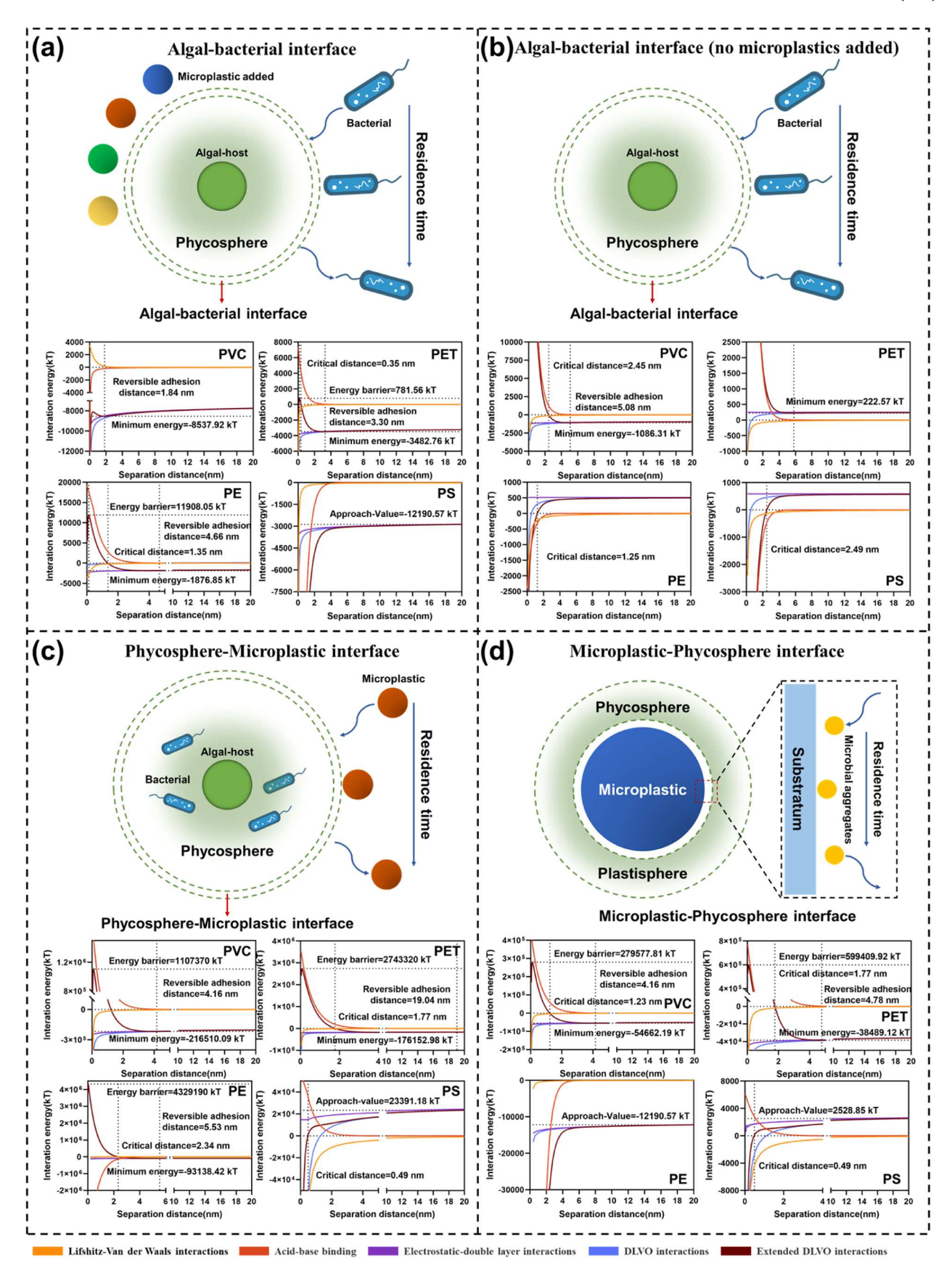


Fig. 4. Profiles of the interaction energies on the separation distance on (a and b) the algal-bacterial and (c and d) microplastic-phycosphere interface with the corresponding schematic presentation.

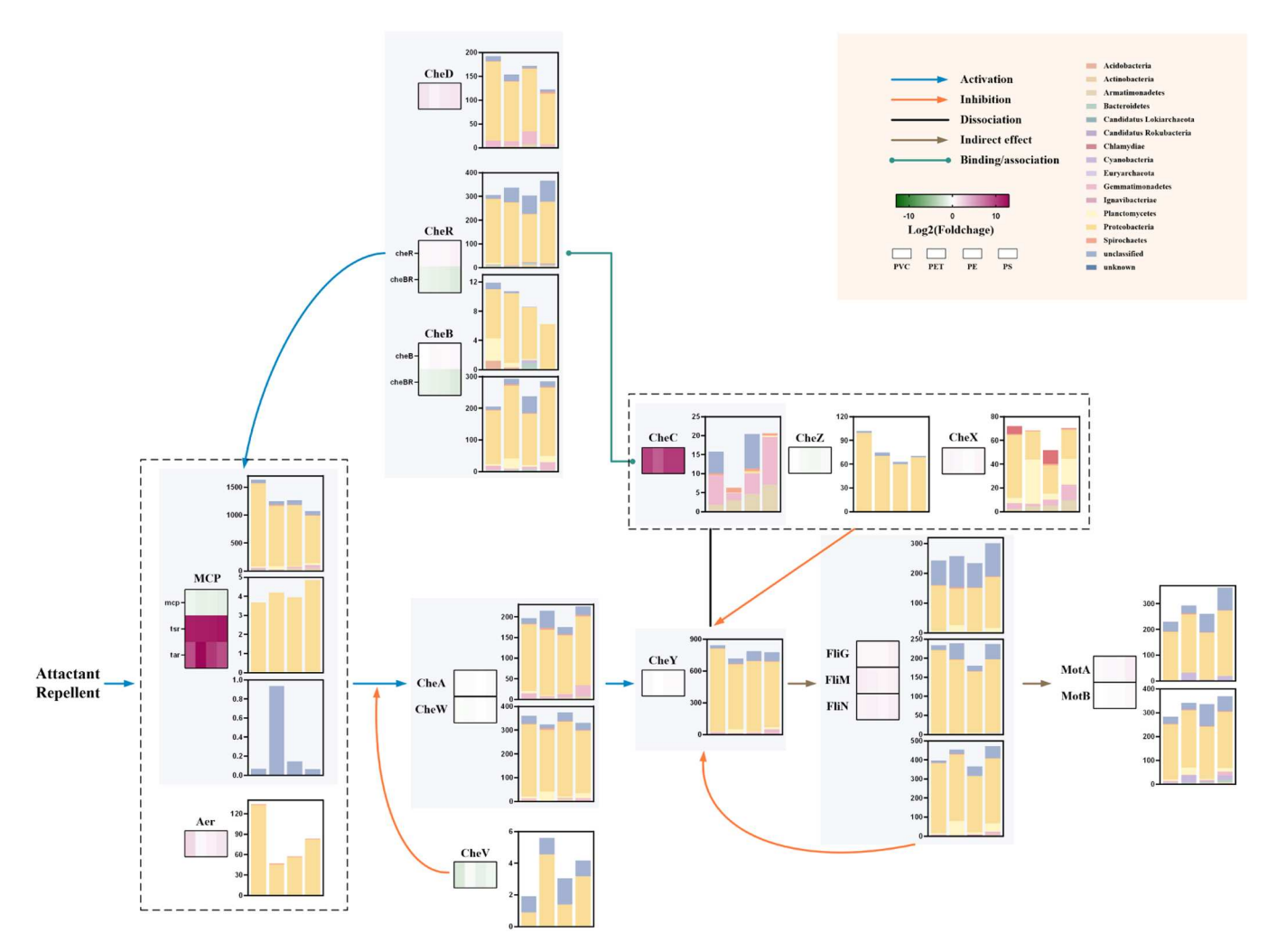


Fig. 5. Comparisons of bacterial chemotaxis (KEGG pathway map02030) between the potential microplastics-degrading algal-bacterial consortia and untreated *Desmodesmus* sp. algal microbiome. The colors of the bar plots indicate the hosts of corresponding functional genes at the phylum level.

## 3.6. Verification of potential microplastics-degrading phycosphere

## 3.6.1. Microplastics degrader MAGs retrieved from the phycosphere

Reconstruction of MAGs originated from PVC, PET, PE and PS microplastics-induced phycosphere microbial communities was supposed to reflected metabolic strategies resulting in microplastic biodegradation. The metagenomic binning recovered 88 high-quality metagenome assembled genomes (completeness >50 % and contamination <10 %). These MAGs were taxonomically appointed to 12 Bacteria phyla (Fig. 6). Furthermore, the potential specific and non-specific genes concerned with PVC, PET, PE and PS degradation were analyzed. A total of 65 MAGs encoded laccase (multi-copper polyphenol oxidoreductase laccase), 14 encoded alkB (alkane 1-monooxygenase), 21 encoded hydrolase (monooxygenase, flavin-binding), 21 encoded dehydrogenase (phenylacetaldehyde dehydrogenase), 46 encoded ligase (phenylacetate-CoA ligase), 32 encoded hydrolases (acting on ester bonds), 73 encoded esterase, 4 encoded mono(ethylene terephthalate) hydrolase (MHETase), analyzed to assess the completeness of the proposed microplastics biodegradation pathway (Fig. 6). Genes involved in the transformation and mineralization of intermediates were also identified based on the presumed degradation process (Figure S10). Unique code of terephthalate 1,2-dioxygenase oxygenase, reductase and dehydrogenase (tphA and tphB) were identified in MAG36, associated with Hydrogenophaga genus. 65 retrieved MAGs were both annotated with alcohol, aldehyde dehydrogenase and acyl-CoA synthetase.

Among the retrieved MAGs, the MAG73, associated with the family

Cyclobacteriaceae and annotated as *alkB*, was the most abundant MAG in the PVC, PET and PE induced phycosphere (mean  $45.52\pm2.38$  %,  $35.87\pm0.41$  % and  $73.50\pm3.87$  % for the counterparts), elaborating the activity in oxidation of alkanes after polymer depolymerization. In contrast, the predominated MAGs (108, 43, 12 and 152) encoding laccase, remained relative homogeneity in PS-treatment. Specially, MAG  $108~(20.80\pm1.10~\%)$  encoded an extra phenylacetyl coenzyme A ligase, assisting phenylacetyl coenzyme A with TCA-cycle. Given the aspecific distribution of presumptive enzymes in different microorganism, biodegradation of polymers in phcosphere represented the interorganism association in symbiotic system, which is consistent with the previous descriptions (Giacomucci et al., 2020; Vargas-Suárez et al., 2019; Zafar et al., 2013).

### 3.6.2. Prediction of the induced pathway in phycosphere

According to the evidence provided by the algal-bacterial consortia genomes and functional groups variation on microplastics, putative degradation processes of these polymers was proposed, including biodegradation and photochemical behaviors (Fig. 7).

The degradation mechanism of PVC-MPs was extremely intricate for the linear long-chain (Das et al., 2012). PVC chain was primarily oxidized and fragmentized into aliphatic primary alcohols (e.g., dodecanol, tetrodecanol and hexadecanol), catalyzed by laccase or other nonspecific lignin degrading system, followed with the further oxidation to the corresponding aldehydes and fatty acids (e.g., dodecanic, myristic and palmitic acid) via the dehydrogenase in the cytoplasm. Then the

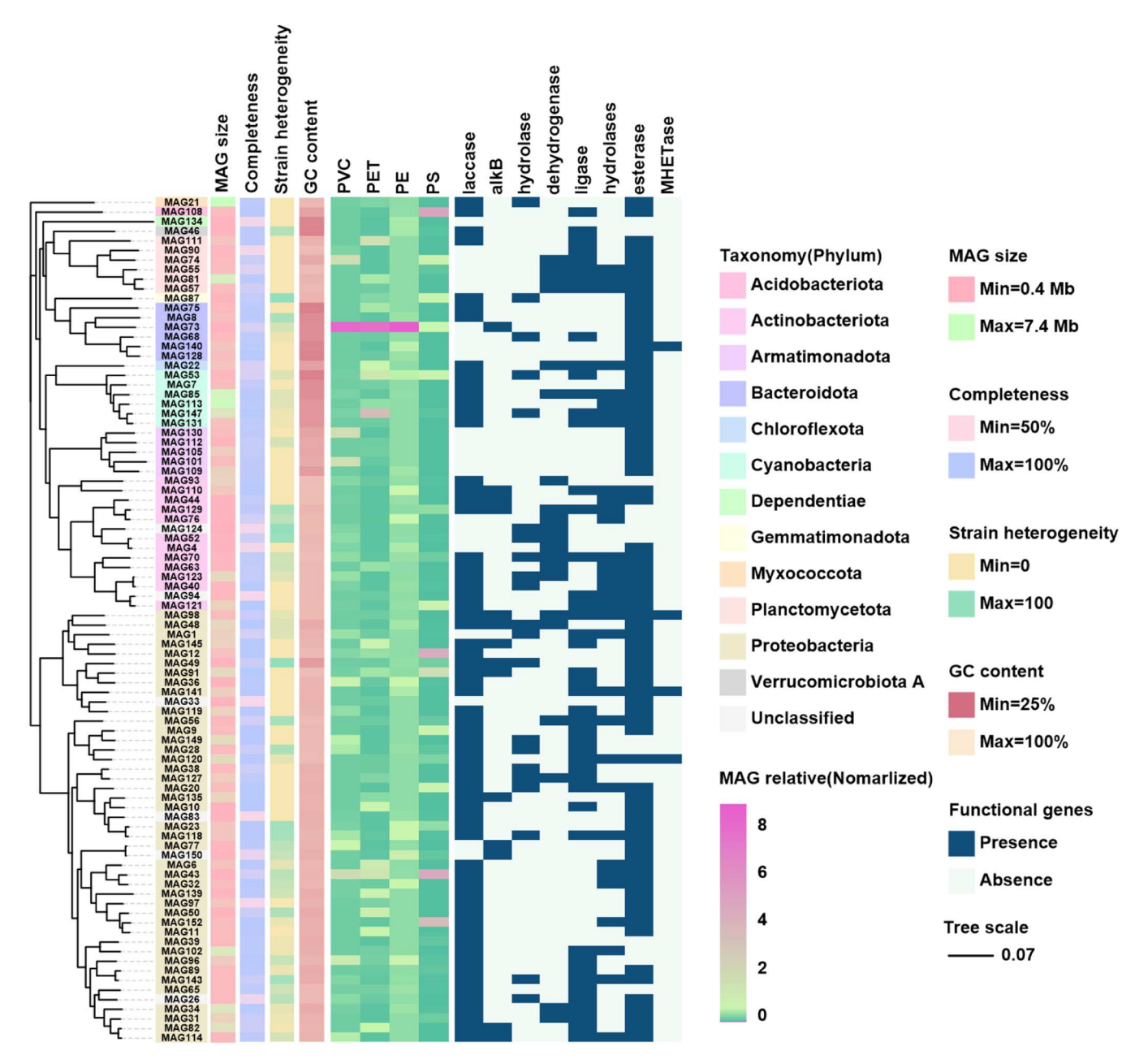


Fig. 6. Reconstruction of the MAGs in the form a phylogenetic tree from microplastic-induced algal-bacterial microbiome.

acids participated in the subsequent mineralization steps containing acyl-CoA synthesis, beta-oxidation, and TCA cycle. However, as the identification of C=O and C-O-C stretch on PVC treated,  $\bullet$ OH radicals generated by the photochemical behavior was suggested to attacked the -Cl, forming the ester group and eventually mineralized similarly.

With the non-detection of PETase (Ioakeimidis et al., 2016; Moog et al., 2019) and the detection of MHETase (Ioakeimidis et al., 2016), illumination and unrecorded hydrolasea or esterase acting on the ester bond, were assumed to initialize the PET degradation procerss, generating mono (2-hydroxyethyl) terephthalate terephthalic acid (MHET) and bis (2-hydroxyethyl) terephthalate (BHET). These intermediate products were hydrolyzed into terephthalic acid and ethylene glycol (Ronkvist et al., 2009). Genes encoding *tphA* and *tphB* involved in the following biodegradation mechanism.

Laccase activated in the depolymerization of PE, facilitating the transport of products (alkanes) into cytoplasm (Gómez-Méndez et al., 2018; Santo et al., 2013). Monooxygenase contributed to the succeeding

intracellular alkane biodegradation and mineralization (Gyung Yoon et al., 2012). Alternatively, produced reactive species under illumination resulted in the C-H bond rupture and oxidation (Jiang et al., 2021).

Extracellular esterase was supposed to capacitate the cleavage of polymer chains and the yield of styrene. Inspired by previous studies (Tischler et al., 2009), styrene oxide and phenyl acetaldehyde were produced via styrene monooxygenase and styrene oxide isomerase, respectively. Since the genes encoded these enzymes were absent in the MAGs/genomes, we suggested alternative pathway. phenyl acetaldehyde was formed via reactive species under irradiation (Zhu et al., 2019) and transported into cytoplasm, and then transformed into phenylacetyl coenzyme A stimulated by phenylacetyl coenzyme A ligase.

Of further note, our co-culture system to microplastics under light irradiation illuminated how microplastics responses are governed by the combination of enzymes catalysis in vivo and in vitro (Amobonye et al., 2021), heteroaggregation as well as photoaging-mediated free radicals (Zhou et al., 2021; Zhu et al., 2019). In real-field wastewater treatment,

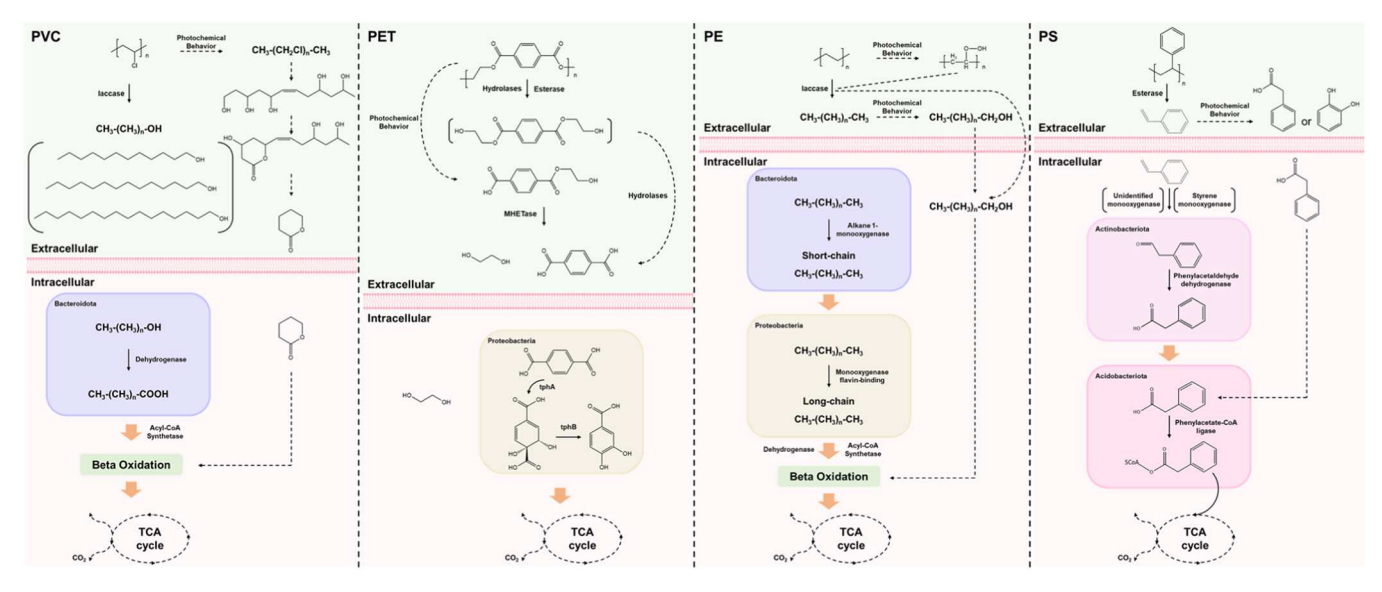


Fig. 7. Potential microplastics degradation pathway in phycosphere.

the algal-bacteria interaction occurred in a turbulence environment, shaping the size of phycosphere, instead of quiescent case (Seymour et al., 2017), thus, hydraulic stress is another major issue for the microenvironment. In the current study, Chlamydiales unclassified genera outcompeted in PVC and PE-induced consortia (Fig. 1f), while was inoperative for biodegradation (Fig. 6). It's instructive to establishing synthetic communities within reductionist approaches to specific removal or inhibition of superfluous strains and populations (Vorholt et al., 2017). Also, the persistence of the ubiquitous and autochthonous algal-bacterial ecological system was confirmed, considering biodegradation reaction temperature occurred at above 30° (Amobonye et al., 2021), which imposing restrictions on the larger platform applications. Herewith, algae-bacterial synergistic system is promising to applied in WWTPs to eliminate microplastics contamination as a third level. Given the speculation, it is essential to conduct future experimental verification on de facto wastewater reuse.

## 4. Conclusion

The current study selected and enriched the Desmodesmus-associated microbiomes to degrade microplastics contamination and authenticated the potentiality through comprehensive evaluation of involved enzymes and interaction between protagonists. Widely applicable degradation pathways of PVC, PET, PE and PS including enzymatic catalysis and photochemical behavior were predicted to open up new opportunities in research with regard to the transformation fate of natural microplastic pollution. Additionally, the organism response to derived DOM and reciprocal yet reversible encounters in phycosphere under microplastic stress indagated herein, illuminated the ecological interface for algalbacteria relationships. Isolation and analysis of the intricacies in the phycosphere will contribute to providing more rigorous insights into the fundamental workings of aquatic ecosystems. Consequently, Desmodesmus-host algal-bacterial symbiotic system could be employed to treat common synthetic microplastic wastes as a frontline photosynthetic organism in the microplastic catastrophe.

### Appendix A. Supplementary data

E-supplementary data for this work can be found in e-version of this paper online.

### CRediT authorship contribution statement

Xuan Fan: Writing – original draft, Visualization, Methodology, Investigation, Data curation, Conceptualization. Lingyu Kong: Validation, Data curation. Jingyi Wang: Methodology, Investigation. Yixiao Tan: Software. Xiangyang Xu: Supervision, Project administration. Mengyan Li: Writing – review & editing, Project administration. Liang Zhu: Supervision, Project administration.

### Declaration of competing interest

The authors declare that they have no known competing financial interests or personal relationships that could have appeared to influence the work reported in this paper.

### Data availability

Data will be made available on request.

### Acknowledgements

This work was supported by the Zhejiang Province Science and Technology Projects (2023C03131&2024C03234), National Science Foundation (NSF, CBET-1903597) and the US Department of Agriculture (USDA, NIFA-2019–67020–30475).

## Supplementary materials

Supplementary material associated with this article can be found, in the online version, at doi:10.1016/j.watres.2024.122064.

### References

 Absolom, D.R., Lamberti, F.V., Policova, Z., Zingg, W.J., Neumann, A.W., 1983. Surface thermodynamics of bacterial adhesion. Appl. Environ. Microbiol. 46 (1), 90–97.
 Amaral-Zettler, L.A., Zettler, E.R., Mincer, T.J., 2020. Ecology of the plastisphere. Nat. Rev. Microbiol. 18 (3), 139–151.

Amin, S.A., Parker, M.S., Armbrust, E.V., 2012. Interactions between diatoms and bacteria. Microbiol. Mol. Biol. Rev. 76 (3), 667–684.

Amobonye, A., Bhagwat, P., Singh, S., Pillai, S., 2021. Plastic biodegradation: frontline microbes and their enzymes. Sci. Total. Environ. 759, 143536.

Andrady, A.L., 2017. The plastic in microplastics: a review. Mar. Pollut. Bull. 119 (1), 12–22.

- Auta, H.S., Emenike, C.U., Jayanthi, B., Fauziah, S.H., 2018. Growth kinetics and biodeterioration of polypropylene microplastics by Bacillus sp. and Rhodococcus sp. isolated from mangrove sediment. Mar. Pollut. Bull. 127, 15–21.
- Banerjee, S., Schlaeppi, K., van der Heijden, M.G.A., 2018. Keystone taxa as drivers of microbiome structure and functioning. Nat. Rev. Microbiol. 16 (9), 567–576.
- Carniello, V., Peterson, B.W., van der Mei, H.C., Busscher, H.J., 2018. Physico-chemistry from initial bacterial adhesion to surface-programmed biofilm growth. Adv. Colloid Interface Sci. 261 (2018), 1–14.
- Chao, Y., Zhang, T., 2011. Probing roles of lipopolysaccharide, type 1 fimbria, and colanic acid in the attachment of Escherichia coli strains on inert surfaces. Langmuir. 27 (18), 11545–11553.
- Cheng, Y.R., Wang, H.Y., 2022. Highly effective removal of microplastics by microalgae Scenedesmus abundans. Chem. Eng. J. 435, 135079.
- Colin, R., Sourjik, V., 2017. Emergent properties of bacterial chemotaxis pathway. Curr. Opin. Microbiol. 39, 24–33.
- Cremer, J., Honda, T., Tang, Y., Wong-Ng, J., Vergassola, M., Hwa, T., 2019. Chemotaxis as a navigation strategy to boost range expansion. Nature 575 (7784), 658–663.
- Das, G., Bordoloi, N.K., Rai, S.K., Mukherjee, A.K., Karak, N., 2012. Biodegradable and biocompatible epoxidized vegetable oil modified thermostable poly(vinyl chloride): thermal and performance characteristics post biodegradation with Pseudomonas aeruginosa and Achromobacter sp. J. Hazard. Mater. 209-210, 434–442.
- Di Cesare, A., Sathicq, M.B., Sbaffi, T., Sabatino, R., Manca, D., Breider, F., Coudret, S., Pinnell, L.J., Turner, J.W., Corno, G., 2024. Parity in bacterial communities and resistomes: microplastic and natural organic particles in the Tyrrhenian Sea. Mar. Pollut. Bull. 203, 116495.
- Dubois, M., Gilles, K.A., Hamilton, J.K., Rebers, P.A., Smith, F., 1956. Colorimetric method for determination of sugars and related substances. Anal. Chem. 28 (3), 350–356.
- Edo, C., González-Pleiter, M., Leganés, F., Fernández-Piñas, F., Rosal, R., 2020. Fate of microplastics in wastewater treatment plants and their environmental dispersion with effluent and sludge. Environ. Pollut. 259, 113837.
- Feng, L.J., Sun, X.D., Zhu, F.P., Feng, Y., Duan, J.L., Xiao, F., Li, X.Y., Shi, Y., Wang, Q., Sun, J.W., Liu, X.Y., Liu, J.Q., Zhou, L.L., Wang, S.G., Ding, Z., Tian, H., Galloway, T. S., Yuan, X.Z., 2020. Nanoplastics promote microcystin synthesis and release from cyanobacterial Microcystis aeruginosa. Environ. Sci. Technol. 54 (6), 3386–3394.
- Flemming, H.C., Wingender, J., 2010. The biofilm matrix. Nat. Rev. Microbiol. 8 (9), 623–633.
- Freeman, S., Booth, A.M., Sabbah, I., Tiller, R., Dierking, J., Klun, K., Rotter, A., Ben-David, E., Javidpour, J., Angel, D.L., 2020. Between source and sea: the role of wastewater treatment in reducing marine microplastics. J. Environ. Manage. 266, 110642.
- Giacomucci, L., Raddadi, N., Soccio, M., Lotti, N., Fava, F., 2020. Biodegradation of polyvinyl chloride plastic films by enriched anaerobic marine consortia. Mar. Environ. Res. 158, 104949.
- Gómez-Méndez, L.D., Moreno-Bayona, D.A., Poutou-Piñales, R.A., Salcedo-Reyes, J.C., Pedroza-Rodríguez, A.M., Vargas, A., Bogoya, J.M., 2018. Biodeterioration of plasma pretreated LDPE sheets by Pleurotus ostreatus. PLoS. One 13 (9), e0203786.
- Gonzalez-Fernandez, C., Toullec, J., Lambert, C., Le Goic, N., Seoane, M., Moriceau, B., Huvet, A., Berchel, M., Vincent, D., Courcot, L., Soudant, P., Paul-Pont, I., 2019. Do transparent exopolymeric particles (TEP) affect the toxicity of nanoplastics on Chaetoceros neogracile? Environ. Pollut. 250, 873–882.
- Gyung Yoon, M., Jeong Jeon, H., Nam Kim, M., 2012. Biodegradation of polyethylene by a soil bacterium and AlkB cloned recombinant cell. Int. Biodeterior. Biodegrad. 03 (04), 1000144.
- Hahn, M.W., O'Melia, C.R, 2004. Deposition and reentrainment of brownian particles in porous media under unfavorable chemical conditions: some concepts and applications. Environ. Sci. Technol. 38 (1), 210–220.
- Huang, S., Zhang, B., Liu, Y., Feng, X., Shi, W., 2022a. Revealing the influencing mechanisms of polystyrene microplastics (MPs) on the performance and stability of the algal-bacterial granular sludge. Bioresour. Technol. 354, 127202.
- Huang, Z., Chen, C., Liu, Y., Liu, S., Zeng, D., Yang, C., Huang, W., Dang, Z., 2022b. Influence of protein configuration on aggregation kinetics of nanoplastics in aquatic environment. Water. Res. 219, 118522.
- Ioakeimidis, C., Fotopoulou, K.N., Karapanagioti, H.K., Geraga, M., Zeri, C., Papathanassiou, E., Galgani, F., Papatheodorou, G., 2016. The degradation potential of PET bottles in the marine environment: An ATR-FTIR based approach. Sci. Rep. 6 (1), 23501.
- Jackrel, S.L., Yang, J.W., Schmidt, K.C., Denef, V.J., 2021. Host specificity of microbiome assembly and its fitness effects in phytoplankton. ISMe J. 15 (3), 774–788.
- Ji, Y., Liu, J., Wang, C., Zhang, F., Xu, X., Zhu, L., 2023. Stability improvement of aerobic granular sludge (AGS) based on Gibbs free energy change (ΔG) of sludge-water interface. Water. Res. 240, 120059.
- Jia, J., Liu, Q., Wu, C., 2023. Microplastic and antibiotic proliferated the colonization of specific bacteria and antibiotic resistance genes in the phycosphere of Chlorella pyrenoidosa. J. Hazard. Mater. 455, 131618.
- Jiang, R., Lu, G., Yan, Z., Liu, J., Wu, D., Wang, Y., 2021. Microplastic degradation by hydroxy-rich bismuth oxychloride. J. Hazard. Mater. 405, 124247.
- Jung, M.R., Horgen, F.D., Orski, S.V., Rodriguez, C.V., Beers, K.L., Balazs, G.H., Jones, T. T., Work, T.M., Brignac, K.C., Royer, S.J., Hyrenbach, K.D., Jensen, B.A., Lynch, J.M, 2018. Validation of ATR FT-IR to identify polymers of plastic marine debris, including those ingested by marine organisms. Mar. Pollut. Bull. 127, 704–716.
- Kay, P., Hiscoe, R., Moberley, I., Bajic, L., McKenna, N., 2018. Wastewater treatment plants as a source of microplastics in river catchments. Environ. Sci. Pollut. Res. 25 (20), 20264–20267.

Kim, H., Kimbrel, J.A., Vaiana, C.A., Wollard, J.R., Mayali, X., Buie, C.R., 2022. Bacterial response to spatial gradients of algal-derived nutrients in a porous microplate. ISMe J. 16 (4), 1036–1045.

- Kim, S., Hoek, E.M.V., 2007. Interactions controlling biopolymer fouling of reverse osmosis membranes. Desalination. 202 (1-3), 333–342.
- Kimbrel, J.A., Samo, T.J., Ward, C., Nilson, D., Thelen, M.P., Siccardi, A., Zimba, P., Lane, T.W., Mayali, X., 2019. Host selection and stochastic effects influence bacterial community assembly on the microalgal phycosphere. Algal. Res. 40, 101489.
- Laganenka, L., Lee, J.W., Malfertheiner, L., Dieterich, C.L., Fuchs, L., Piel, J., von Mering, C., Sourjik, V., Hardt, W.D., 2023. Chemotaxis and autoinducer-2 signalling mediate colonization and contribute to co-existence of Escherichia coli strains in the murine gut. Nat. Microbiol. 8 (2), 204–217.
- Li, X., Chen, L., Mei, Q., Dong, B., Dai, X., Ding, G., Zeng, E.Y., 2018. Microplastics in sewage sludge from the wastewater treatment plants in China. Water. Res. 142, 75–85
- Lin, Y., Wang, L., Xu, K., Huang, H., Ren, H., 2021. Algae biofilm reduces microbederived dissolved organic nitrogen discharges: performance and mechanisms. Environ. Sci. Technol. 55 (9), 6227–6238.
- Liu, G., Jiang, R., You, J., Muir, D.C.G., Zeng, E.Y., 2020. Microplastic impacts on microalgae growth: effects of size and humic acid. Environ. Sci. Technol. 54 (3), 1782–1789.
- Lou, Z., Zhang, Y., Li, Y., Xu, L., 2023. Study on microscopic physical and chemical properties of biomass materials by AFM. J. Mater. Res. Technol. 24, 10005–10026. Matilla, M.A., Krell, T., 2018. The effect of bacterial chemotaxis on host infection and
- pathogenicity. Fems Microbiol. Rev. 42 (1), 40–67.

  Merton, R.K., 1968. The Matthew effect in science. The reward and communication systems of science are considered. Science (1979) 159 (3810), 56–63.
- Milo, R., Jorgensen, P., Moran, U., Weber, G., Springer, M., 2010. BioNumbers—The database of key numbers in molecular and cell biology. Nucleic. Acids. Res. 38 (1), 750–753
- Moog, D., Schmitt, J., Senger, J., Zarzycki, J., Rexer, K.H., Linne, U., Erb, T., Maier, U.G., 2019. Using a marine microalga as a chassis for polyethylene terephthalate (PET) degradation. Microb. Cell Fact. 18 (1), 171.
- Ni, B., Colin, R., Link, H., Endres, R.G., Sourjik, V., 2020. Growth-rate dependent resource investment in bacterial motile behavior quantitatively follows potential benefit of chemotaxis. Proc. Natl. Acad. Sci. 117 (1), 595–601.
- Ou, Q., Xu, Y., Li, X., He, Q., Liu, C., Zhou, X., Wu, Z., Huang, R., Song, J., Huangfu, X., 2020. Interactions between activated sludge extracellular polymeric substances and model carrier surfaces in WWTPs: a combination of QCM-D, AFM and XDLVO prediction. Chemosphere 253 (2020), 126720.
- Park, S.Y., Chao, X., Gonzalez-Bonet, G., Beel, B.D., Bilwes, A.M., Crane, B.R., 2004. Structure and function of an unusual family of protein phosphatases: the bacterial chemotaxis proteins CheC and CheX. Mol. Cell 16 (4), 563–574.
- Phuong, N.N., Zalouk-Vergnoux, A., Poirier, L., Kamari, A., Châtel, A., Mouneyrac, C., Lagarde, F., 2016. Is there any consistency between the microplastics found in the field and those used in laboratory experiments? Environ. Pollut. 211, 111–123.
- Pranzetti, A., Mieszkin, S., Iqbal, P., Rawson, F.J., Callow, M.E., Callow, J.A., Koelsch, P., Preece, J.A., Mendes, P.M., 2013. An electrically reversible switchable surface to control and study early bacterial adhesion dynamics in real-time. Adv. Mater. 25 (15), 2181–2185.
- Raina, J.B., Giardina, M., Brumley, D.R., Clode, P.L., Pernice, M., Guagliardo, P., Bougoure, J., Mendis, H., Smriga, S., Sonnenschein, E.C., Ullrich, M.S., Stocker, R., Seymour, J.R., 2023. Chemotaxis increases metabolic exchanges between marine picophytoplankton and heterotrophic bacteria. Nat. Microbiol. 8 (3), 510–521.
- Ronkvist, Å.M., Xie, W., Lu, W., Gross, R.A., 2009. Cutinase-catalyzed hydrolysis of poly (ethylene terephthalate). Macromolecules. 42 (14), 5128–5138.
- Russell, J.R., Huang, J., Anand, P., Kucera, K., Sandoval, A.G., Dantzler, K.W., Hickman, D., Jee, J., Kimovec, F.M., Koppstein, D., Marks, D.H., Mittermiller, P.A., Nunez, S.J., Santiago, M., Townes, M.A., Vishnevetsky, M., Williams, N.E., Vargas, M.P., Boulanger, L.A., Bascom-Slack, C., Strobel, S.A., 2011. Biodegradation of polyester polyurethane by endophytic fungi. Appl. Environ. Microbiol. 77 (17), 6076–6084.
- Sánchez, C., 2020. Fungal potential for the degradation of petroleum-based polymers: an overview of macro- and microplastics biodegradation. Biotechnol. Adv. 40, 107501.
- Santo, M., Weitsman, R., Sivan, A., 2013. The role of the copper-binding enzyme laccase in the biodegradation of polyethylene by the actinomycete Rhodococcus ruber. Int. Biodeterior. Biodegrad. 84, 204–210.
- Santos, R.G., Machovsky-Capuska, G.E., Andrades, R., 2021. Plastic ingestion as an evolutionary trap: toward a holistic understanding. Science (1979) 373 (6550), 56-60.
- Seymour, J.R., Amin, S.A., Raina, J.B., Stocker, R., 2017. Zooming in on the phycosphere: the ecological interface for phytoplankton-bacteria relationships. Nat. Microbiol. 2, 17065.
- Sjöstedt, J., Koch-Schmidt, P., Pontarp, M., Canbäck, B., Tunlid, A., Lundberg, P., Hagström, Å., Riemann, L., 2012. Recruitment of members from the rare biosphere of marine bacterioplankton communities after an environmental disturbance. Appl. Environ. Microbiol. 78 (5), 1361–1369.
- Smriga, S., Fernandez, V.I., Mitchell, J.G., Stocker, R., 2016. Chemotaxis toward phytoplankton drives organic matter partitioning among marine bacteria. Proc. Natl. Acad. Sci. 113 (6), 1576.
- Song, C., Hu, X., Liu, Z., Li, S., Kitamura, Y., 2020. Combination of brewery wastewater purification and CO2 fixation with potential value-added ingredients production via different microalgae strains cultivation. J. Clean Prod. 268.
- Strokal, M., Bai, Z., Franssen, W., Hofstra, N., Koelmans, A.A., Ludwig, F., Ma, L., van Puijenbroek, P., Spanier, J.E., Vermeulen, L.C., van Vliet, M.T.H., van Wijnen, J.,

Kroeze, C., 2021. Urbanization: an increasing source of multiple pollutants to rivers in the 21st century. npj Urban. Sustain. 1 (1), 24.

- Sun, X., Chen, Z., Kong, T., Chen, Z., Dong, Y., Kolton, M., Cao, Z., Zhang, X., Zhang, H., Liu, G., Gao, P., Yang, N., Lan, L., Xu, Y., Sun, W., 2022. Mycobacteriaceae mineralizes micropolyethylene in riverine ecosystems. Environ. Sci. Technol. 56 (22), 15705–15717.
- Syranidou, E., Kalogerakis, N., 2022. Interactions of microplastics, antibiotics and antibiotic resistant genes within WWTPs. Sci. Total. Environ. 804, 150141
- Tajima, H., Imada, K., Sakuma, M., Hattori, F., Nara, T., Kamo, N., Homma, M., Kawagishi, I., 2011. Ligand specificity determined by differentially arranged common ligand-binding residues in bacterial amino acid chemoreceptors Tsr and Tar\*. J. Biol. Chem. 286 (49), 42200–42210.
- Tan, Y., Yu, P., Huang, D., Yuan, M.M., Yu, Z., Lu, H., Alvarez, P.J.J., Zhu, L., 2023. Enhanced bacterium-phage symbiosis in attached microbial aggregates on a membrane surface facing elevated hydraulic stress. Environ. Sci. Technol. 57 (45), 17324-17337.
- Thiagarajan, V., Iswarya, V., P, A.J., Seenivasan, R., Chandrasekaran, N., Mukherjee, A, 2019. Influence of differently functionalized polystyrene microplastics on the toxic effects of P25 TiO2 NPs towards marine algae Chlorella sp. Aquat. Toxicol. 207, 208-216
- Tischler, D., Eulberg, D., Lakner, S., Kaschabek Stefan, R., van Berkel Willem, J.H., Schlömann, M., 2009. Identification of a novel self-sufficient styrene monocygenase from rhodococcus opacus 1CP. J. Bacteriol. 191 (15), 4996–5009.
- van der Westen, R., Sjollema, J., Molenaar, R., Sharma, P.K., van der Mei, H.C., Busscher, H.J., 2018. Floating and tether-coupled adhesion of bacteria to hydrophobic and hydrophilic surfaces. Langmuir. 34 (17), 4937–4944.
- van Oss, C.J., 1993. Acid-base interfacial interactions in aqueous media. Colloid Surf. A-Physicochem. Eng. Asp. 78 (93), 1–49.
- Vargas-Suárez, M., Fernández-Cruz, V., Loza-Tavera, H., 2019. Biodegradation of polyacrylic and polyester polyurethane coatings by enriched microbial communities. Appl. Microbiol. Biotechnol. 103 (7), 3225–3236.
- Vorholt, J.A., Vogel, C., Carlström, C.I., Müller, D.B., 2017. Establishing causality: opportunities of synthetic communities for plant microbiome research. Cell Host. Microbe 22 (2), 142–155.
- Wang, J., Wang, Y., Li, X., Weng, Y., Dong, X., Zhao, X., 2022. Comparison on the effectiveness of Fourier transform infrared (FT-IR) and attenuated total reflection Fourier transform infrared (ATR-FT-IR) in characterizing plastics biodegradation by insect larvae. Sci. Total. Environ. 839, 156289.
- Waters, C.N., Zalasiewicz, J., Summerhayes, C., Barnosky, A.D., Poirier, C., Gałuszka, A., Cearreta, A., Edgeworth, M., Ellis, E.C., Ellis, M., Jeandel, C., Leinfelder, R., McNeill, J.R., Richter, D.d., Steffen, W., Syvitski, J., Vidas, D., Wagreich, M., Williams, M., Zhisheng, A., Grinevald, J., Odada, E., Oreskes, N., Wolfe, A.P., 2016.

- The Anthropocene is functionally and stratigraphically distinct from the Holocene. Science (1979) 351 (6269), aad2622.
- Wilkes, R.A., Aristilde, L., 2017. Degradation and metabolism of synthetic plastics and associated products by Pseudomonas sp.: capabilities and challenges. J. Appl. Microbiol. 123 (3), 582–593.
- Woodward, J., Li, J., Rothwell, J., Hurley, R., 2021. Acute riverine microplastic contamination due to avoidable releases of untreated wastewater. Nat. Sustain. 4 (9), 793–802.
- Wu, J., Lu, L., Wang, R., Pan, L., Chen, B., Zhu, X., 2023. Influence of microplastics on the transport of antibiotics in sand filtration investigated by AFM force spectroscopy. Sci. Total. Environ. 873, 162344.
- Wu, Y., Guo, P., Zhang, X., Zhang, Y., Xie, S., Deng, J., 2019. Effect of microplastics exposure on the photosynthesis system of freshwater algae. J. Hazard. Mater. 374, 219–227.
- Xu, L., Liu, J., Meng, J., Cao, Y., Wang, D., Fan, G., Shi, X., Xue, K., 2024. Understanding the anisotropic wettability of spodumene from direct force measurement using AFM and density functional theory calculations. Miner. Eng. 205, 108454.
- Yong, J.J.J.Y., Chew, K.W., Khoo, K.S., Show, P.L., Chang, J.S., 2021. Prospects and development of algal-bacterial biotechnology in environmental management and protection. Biotechnol. Adv. 47, 107684.
- Yoshida, S., Hiraga, K., Takehana, T., Taniguchi, I., Yamaji, H., Maeda, Y., Toyohara, K., Miyamoto, K., Kimura, Y., Oda, K., 2016. A bacterium that degrades and assimilates poly(ethylene terephthalate). Science (1979) 351 (6278), 1196–1199.
- Yuan, S., Gao, M., Ma, H., Afzal, M.Z., Wang, Y.K., Wang, M., Xu, H., Wang, S.G., Wang, X.H., 2018. Qualitatively and quantitatively assessing the aggregation ability of sludge during aerobic granulation process combined XDLVO theory with physicochemical properties. J. Environ. Sci. 67 (2018), 154–160.
- Zafar, U., Houlden, A., Robson Geoffrey, D., 2013. Fungal communities associated with the biodegradation of polyester polyurethane buried under compost at different temperatures. Appl. Environ. Microbiol. 79 (23), 7313–7324.
- Zettler, E.R., Mincer, T.J., Amaral-Zettler, L.A., 2013. Life in the "plastisphere": microbial communities on plastic marine debris. Environ. Sci. Technol. 47 (13), 7137–7146.
- Zhang, Z., Yu, Z., Dong, J., Wang, Z., Ma, K., Xu, X., Alvarezc, P.J.J., Zhu, L., 2018. Stability of aerobic granular sludge under condition of low influent C/N ratio: correlation of sludge property and functional microorganism. Bioresour. Technol. 270, 391–399.
- Zhou, S., Liao, Z., Zhang, B., Hou, R., Wang, Y., Zhou, S., Zhang, Y., Ren, Z.J., Yuan, Y., 2021. Photochemical behavior of microbial extracellular polymeric substances in the aquatic environment. Environ. Sci. Technol. 55 (22), 15090–15099.
- Zhu, K., Jia, H., Zhao, S., Xia, T., Guo, X., Wang, T., Zhu, L., 2019. Formation of environmentally persistent free radicals on microplastics under light irradiation. Environ. Sci. Technol. 53 (14), 8177–8186.